Journal of Petroleum Exploration and Production Technology
https://doi.org/10.1007/s13202-023-01672-9

ORIGINAL PAPER-PRODUCTION ENGINEERING

Experimental quantification of the performance of a horizontal multi-pipe bulk separator of water and oil with crude spiking

Hamidreza Asaadian[1] · **Milan Stanko**[1]

Received: 9 August 2022 / Accepted: 7 July 2023

Abstract

Subsea water separation with pipe separators is crucial for ensuring efficient and environmentally responsible extraction of oil and gas from the seabed. In this study, in a process called as "crude oil spiking," two concentrations of crude oil (e.g., 185 and 400 ppm) are added to Exxsol D60 to mimic the separation characteristics of real crude oil mixtures in a multi-parallel pipe separator. The pipe separator performance for water–oil bulk separation such as separation efficiency, water cut ratio, the flow pattern at the separator inlet, and the thickness and evolution of the fluid layers in the separator is evaluated and compared to the values when operating with unspiked Exxsol D60. Crude oil spiking significantly reduces the efficiency of the pipe separator and reduces the water cut ratio for oil continuous regimes (low water cuts) up to 49%. Water continuous regimes with water fractions 90% have the highest efficiency values; thus, these are not affected significantly by crude oil spiking. With crude spiking, the flow regime dispersion of oil in water and water in oil (Dw/o + Do/w) occupies more area in the flow pattern map than unspiked Exxsol D60. It was observed through visual inspection that crude oil spiking induces a thicker and more stable emulsion in higher flow rates (e.g., 700 L/min). Therefore, the spiked mixture needs more time to separate. The findings of this study can help in a better understanding of the applicability of pipe separators and the usage of spiked oils to extrapolate experimental results to real field conditions.

✉ Hamidreza Asaadian
hamidreza.asaadian@ntnu.no

[1] Department of Geoscience and Petroleum, Norwegian University of Science and Technology, Trondheim, Norway

Published online: 22 July 2023

Graphical abstract

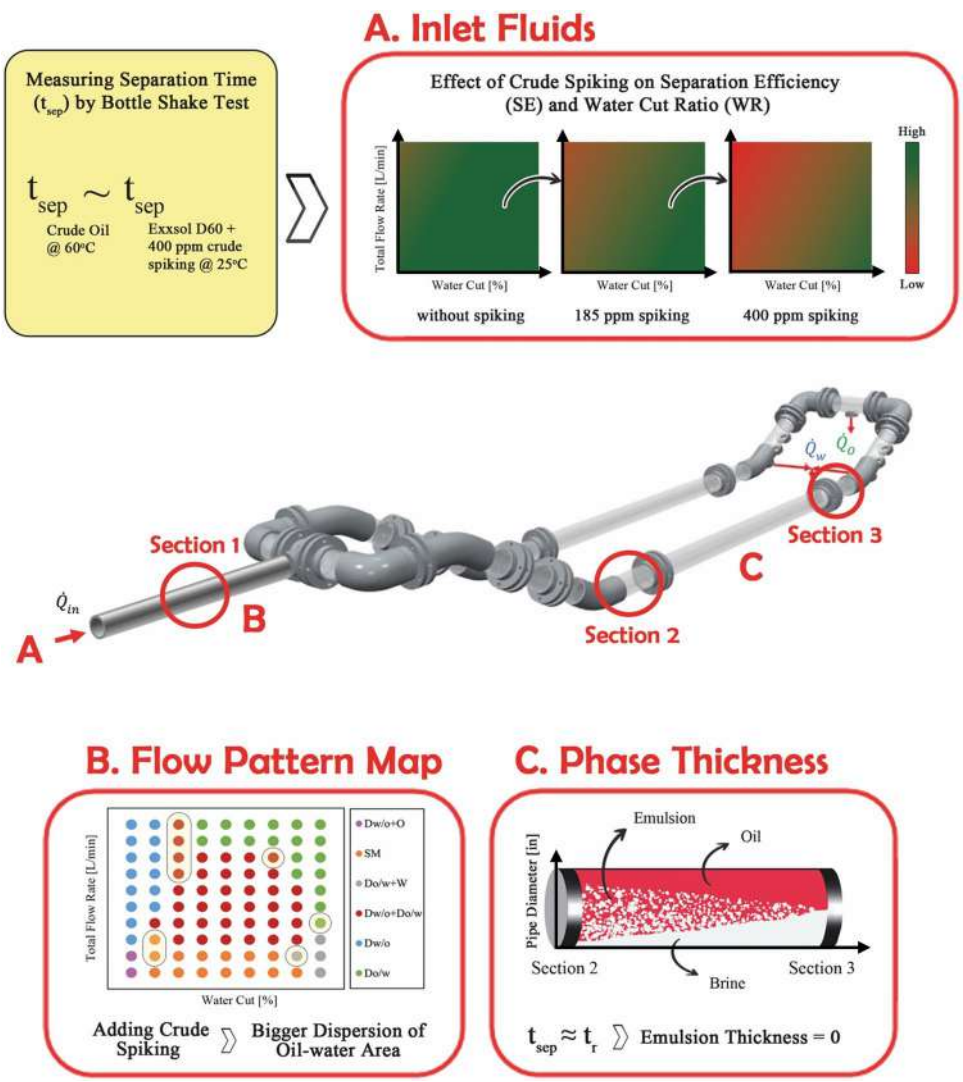

Keywords Multi-parallel pipe separator (MPPS) · Crude oil spiking · Separation efficiency · Water cut ratio · Flow pattern · Fluid layer thickness

Abbreviations

BC	Brine characteristic
ER	Extraction rate
MPPS	Multi-parallel pipe separator
NCS	Norwegian continental shelf
HPS	Horizontal pipe separator

Variables

Q	Flow rate (L/min)
V	Volume (m^3)
WC	Water cut
t	Time (s)

Greek symbols

ρ	Density (kg/m^3)
ε	Separation efficiency

Subscripts

i	Initial
in	Interfacial
o	Oil
r	Residence
sep	Separation
t	Total
w	Water

Introduction

One of the undesirable by-products of oil production is associated water. Most oil fields experience a gradual increase in water produced with the oil during the field life (Asaadian and Stanko 2023). Fields which initially produce only oil may end up producing as much as 90% water in the later stages of field life (Bringedal et al. 1999). It has been reported that the global produced associated water is about 250 million bpd which is three times more than global hydrocarbon production (Fakhru'l-Razi et al. 2009; Hannisdal et al. 2012). Meanwhile, it was reported that in 2016 the Norwegian Continental Shelf (NCS) had a water production of 181 million standard cubic meters. This amount of water production corresponds to twice the oil production (Oil and Gas Association 2016). The conventional approach to deal with water production is to design topside facilities with a capacity equal to the maximum estimated water production rate expected during the field's life (da Silva et al. 2013). However, it often occurs that water production reaches the processing capacity; then, it is often necessary to reduce oil production, which entails a significant loss of revenue (Skjefstad and Stanko 2017).

The separation of produced water at seabed would offer several benefits like more compact topside installations, smaller and fewer pipes and risers, reduced usage of chemicals, reduced backpressure on the reservoir (Bringedal et al. 1999). The key benefits of subsea separation can be outlined as three separate aspects. (1) Subsea separation of produced water can reduce the load on topside capacity and facilities, allowing for prolonged, increased production and avoiding bottlenecking. (2) Subsea water separation also reduces the fluid pressure losses from seabed to topside, thus enabling more energy-efficient production, extension of plateau period or increase in hydrocarbon rates (Skjefstad and Stanko 2019). (3) Finally, separation close to the well means less mixing and agitation, reducing dispersion formation and allowing for better separation (Skjefstad and Stanko 2018).

Therefore, several water treatment solutions have been recently applied to separate water at seabed before transferring to topside processing facilities (Skjefstad and Stanko 2019). Existing solutions can be categorized into two groups of design, the gravity vessel and compact gravity vessel approach of Troll C and Tordis and the pipe separator strategy used at Marlim, Saipem's SpoolSep and horizontal pipe separator (HPS) (see Fig. 1) (Fantoft et al. 2006; Hannisdal et al. 2012; Horn et al. 2003; Orlowski et al. 2012; Pereyra et al. 2013; Skjefstad and Stanko 2018).

In gravity-based vessels, the residence time is high and fluid velocities are low such that it allows droplets and bubbles to travel from vertically toward the phase layers (Skjefstad and Stanko 2017). However, due to the high residence time (1–4 min) required they usually have huge diameter, footprint, weight and cost (Skjefstad and Stanko 2017; Van Vu et al. 2009).

The use of pipe sections as separators has been evaluated and verified over the last decades by StatoilHydro (Grave and Olson 2014; Sagatun et al. 2008) and ExxonMobil (Gramme and Haukom 2009). The diameter in this kind of separators is considerably smaller when compared to gravity or compact gravity vessels. The reduction in diameter provides a shorter droplet traveling distance which consequently results in lower residence time. Besides, it makes this design more attractive for deep-water installations because thinner walls can be used which reduces overall weight (Shaiek and Grandjean 2015). However, the installed pipe separators are too long like Marlim with a pipe length of 60 m, which makes them heavy installation (Capela Moraes et al. 2012; de Oliveira et al. 2013; Orlowski et al. 2012).

To make subsea water separation more affordable, the primary area of effort is to decrease the size and weight of separator modules. Assuring a high flow capacity and operational envelope for deep-water installations is the second key area. To lower the overall cost of upcoming projects, the third priority area entails creating standardized solutions that can be qualified for a variety of field operating circumstances. Utilizing modularization and adaptive design strategies, which can ensure the mentioned focus areas, is the fourth emphasis area (Fakhru'l-Razi et al. 2009; Gupta et al. 2017; Skjefstad and Stanko 2017).

Based on the results by Rivera et al. (2008), Skjefstad and Stanko (2017) proposed a separator design for bulk

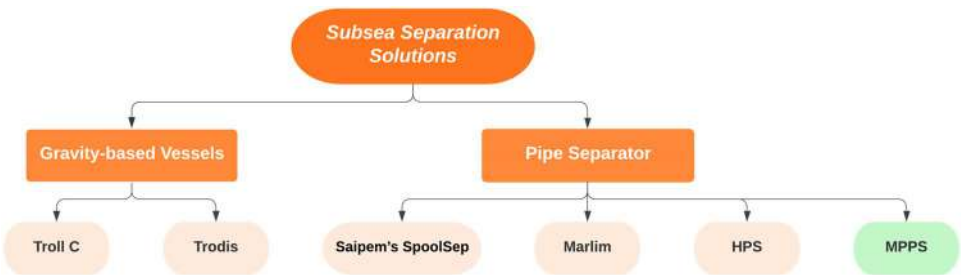

Fig. 1 Classification of existing subsea separation solutions

oil–water separation using multiple parallel branches named the multiple parallel pipe separator (MPPS) to satisfy all mentioned focus areas (Skjefstad and Stanko 2018; Skjefstad and Stanko 2019; Skjefstad et al. 2020). The concept utilizes multiple pipes in parallel, offering reduced settling times and a more compact, modularized and adaptive separator design compared to existing subsea bulk-water separator installations (Skjefstad et al. 2020). Skjefstad (2020) built and tested a prototype and evaluated the effect of design features on separation efficiency and the effect of surfactants and inlet choking on the separation efficiency (Stanko and Golan 2015).

This work is a continuation of previous work performed at NTNU and the Department of Geoscience and Petroleum on bulk oil–water separation in pipes. The gaps addressed in this study are the following:

- Bulk oil–water pipe separators have clear advantages over large gravity vessels, especially for subsea and deep-water applications. However, their adoption has not been fully realized in real oil and gas assets due to uncertainties related to their performance and design. This study provides experimental performance data aiming to reduce uncertainty when operating with real fluids.
- Further advancement of the technology readiness level of the MPPS concept.
- A common limitation of test facilities for multiphase flow and separation is that model oils are frequently employed instead of real crudes, thus casting doubts about the applicability and extrapolation of results to real field conditions. This study provides experimental performance data to quantify how different the performance is when operating with model and real fluids.

Several methods have been used in the past to make model oil–water systems more realistic in terms of separation performance, for example, usage of mixture of mineral oils and different stabilizers such as oil-soluble surfactants and hydrophobic nanoparticles. Initially, mixtures of kerosene and silicon oils were used, and later mixtures of Primol 352 and Exxsol D60 with or without SPAN® 83 (sorbitan sesquioleate), Aerosil® R104 (hydrophobic-fumed silica nanoparticles) and myristic acids were used (Brown and Pitt 1972; Calabrese et al. 1986; Fossen and Schümann 2017; Keleşoğlu et al. 2015). Lately, blends of crude oil with mineral oil have been used to vary the bulk viscosity without significant changes in interfacial properties (Boxall et al. 2010).

This study offers a compact, standardized, adaptive and cost-effective pipe separator suitable for subsea applications. The study's findings indicate the strengths and weaknesses of the suggested separator and shed light on how the MPPS performs in actual field situations. However, it should be noted that the offered separator is only suitable for separating oil and water and is not designed to handle significant amounts of gas. Additionally, due to the limited space available at subsea facilities station, the MPPS concept has a length limitation of 7 m (Skjefstad and Stanko 2017). Moreover, the model oil used in the experiments was spiked with specific crude oil properties and may not provide the exact results when the MPPS concept operates with different crude system.

In this work, an experimental study was conducted to quantify the performance of a multi-parallel pipe separator (MPPS) for bulk separation of water–oil. First, to mimic the separation characteristics of real crude oil mixtures, small quantities of real crude are added to the Exxsol D60, a process called "crude oil spiking." Several bottle tests are performed to find the optimum crude concentration as spiking agent. Then, after using two different concentrations of crude oil (e.g., 185 and 400 ppm), the effect of crude concentration on the separation characteristics such as separation efficiency, water cut ratio, flow pattern at separator inlet and thickness and evolution of the fluid layers in the separator is investigated. Results were compared against the values when operating with unspiked Exxsol D60. Finally, a new concept as brine characteristic is introduced to ensure efficient oil–water separation in MPPS.

Methods and materials

MPPS experimental setup

The process and instrumentation diagram of the experimental facilities is shown in Fig. 2. There is a large storage tank (total liquid capacity of 6 m^3) to provide base separation, two small and two large centrifugal pumps, pipes, valves and pressure and flowmeters. Single-phase water and oil streams are drained from the storage tank tap points and then pumped; their flow rates are measured and then merged into a single flowline. The mixture stream then passes via an inlet valve and onto a separator prototype, which separates a water-rich stream from an oil-rich stream. Two flowlines are then used to direct the two separated streams to the storage tank.

Inflow oil and water rates, and water cut are controlled by adjusting the frequency of the pumps. The rates of the separated streams (oil-rich and water-rich) are controlled by gradually opening or shutting the control valves VT.2 and VT.1. Pressure is recorded at the intake and outtakes of the separator, as well as across the inlet valve. The rates and water cuts of the inlet streams are measured and monitored using two Coriolis flowmeters (FT.1, FT.2) installed before the merging point. The flow rate and water cut of the

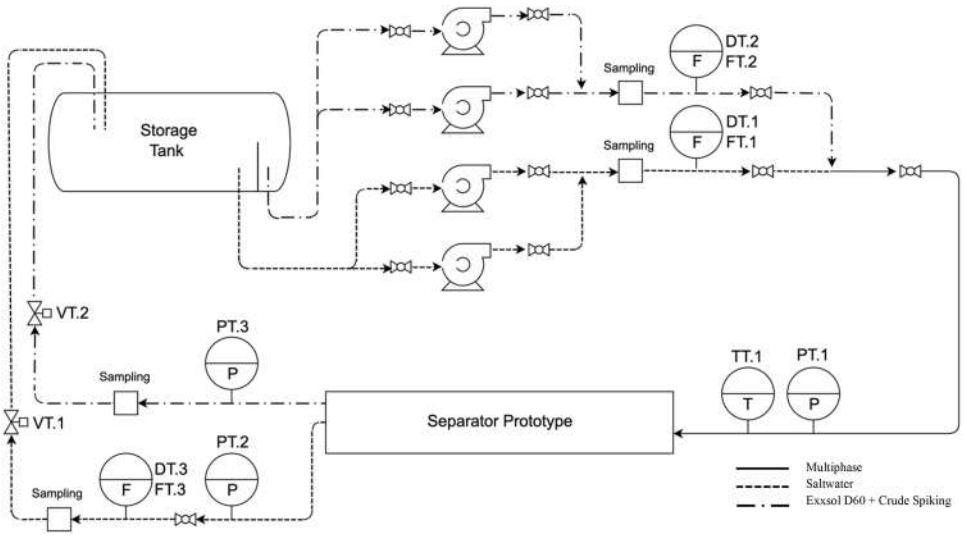

Fig. 2 PI&D of the experimental system setup

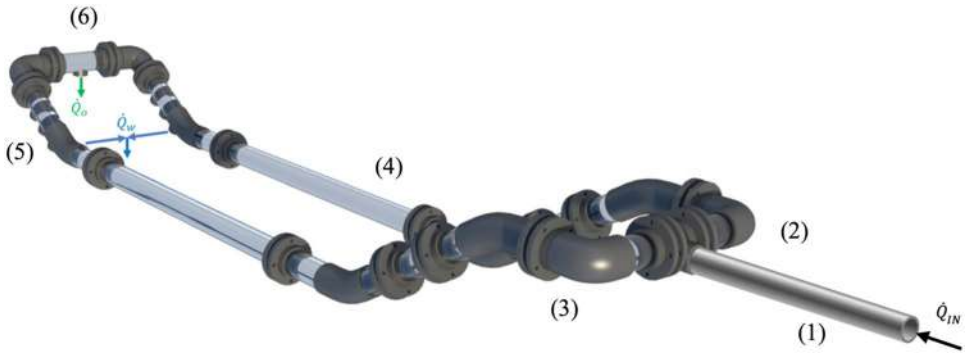

Fig. 3 Prototype of parallel pipe bulk oil–water separator

water-rich stream are monitored and recorded using a Coriolis flowmeter located on the outtake of the water-rich stream.

The separator prototype, which is illustrated in Fig. 3, consists of following parts: (1) a tangential intake to generate pre-separation using centrifugal forces. The heavier phase (salt water) will be forced toward the pipe walls, while the lighter phase (oil) will concentrate in the center. To convert from this annular flow configuration to a stratified configuration, an internal device was placed in the elbow immediately downstream of the T-Section (2). The T-junction header inlet also splits the inlet stream into each branch.

The flow stream then enters a descending pipe Section (3). Originally, this section was added for two reasons: (1) for gas removal using extraction points located at the top of the pipe [similar to the Harp separator used in the Marlim field (Capela Moraes et al. 2012)] and (2) provide pre-separation and establishment of a stratified layer before the horizontal section (Stanko 2014). However, the experiments in this study are performed without any gas extraction.

The flow then enters a horizontal mid-section (4) with a length of 3.5 m and internal diameter 150.6 mm, where the main liquid–liquid separation occurs. This is driven by gravitational forces and density differences. As previously stated, the smaller pipe diameter and horizontal pipe structure enable a short droplet vertical travel distance and hence short residence time is required, allowing the use of short pipe segments. The flow then enters an ascending pipe section where extraction takes place (5). A water-rich stream is extracted from the pipe through a tapping point near the bottom. The oil-rich stream flows up toward the outlet (6).

Table 1 Fluid properties

Fluid	Density [kg/m^3]	Viscosity [cP]
Distilled water w/wt% 3.4 NaCl	1023.7	0.99
Exxsol D60 w/0.015 g/L oil red O	796.2	1.41
Crude oil	939.1	224.01

Materials

Experimental fluids are Exxsol D60 and distilled water with added wt% 3.4 NaCl (da Silva et al. 2013). Small amounts of the colorant Oil Red O ($C_{26}H_{24}N_4O$, for better visualization) and crude oil have been added to the Exxsol D60. A brief overview of fluid properties is presented in Table 1.

To avoid bacterial growth in the storage tank, fluids are drained regularly from the oil–water interface, passed through a filter and a UV-C lamp and sent back to the tank. It was decided to use this method instead of chemical inhibition to avoid any further modification of the properties of the oil–water mixture.

Test matrix

Bottle test

The bottle test is commonly used to determine separation times and study the effect of different chemicals on breaking or separating the emulsions and dispersions. In this work bottle tests are used to determine how much crude must be added to Exxsol D60 to obtain similar separation times for the real crude oil and water at temperature of 60 °C (assumed temperature of the well stream entering the separator). For this purpose, two series of bottle tests were designed. First, a series of experiments were conducted at 60 °C with pure crude oil and salt water for four different water cuts (e.g., 30, 50, 70 and 90%). Next, a second series of experiments was conducted for Exxsol D60 spiked with crude and salt water at ambient temperature (25 °C) with seven different crude oil concentrations (e.g., 200, 300, 400, 500, 600, 700 and 800 ppm) and three water cuts (e.g., 25, 50 and 75%).

The mixture was agitated at 750 rpm for 30 s before allowing time for phase separation. For each sample, the separation process was filmed three times and then analyzed. The results are divided into two time periods. t_{in} illustrates how long it takes for the interface between Exxsol D60 spiked with crude oil and water to stabilize in the container at a certain height after the magnetic mixer has stopped stirring. t_{sep} is the time between the end of mixing and the point where the two layers separate completely (Fig. 4).

A visibility test was performed to ensure crude spiking does not affect the visibility through the transparent pipes. The summary of fixed, study and response variables for the two series of bottle tests is presented in Table 2.

Separation performance test

Separator performance is determined from the flow rate and density measurements of the flow streams entering the separator and the water-rich stream leaving the separator. Additionally, temperature and pressure, lateral pipe pictures

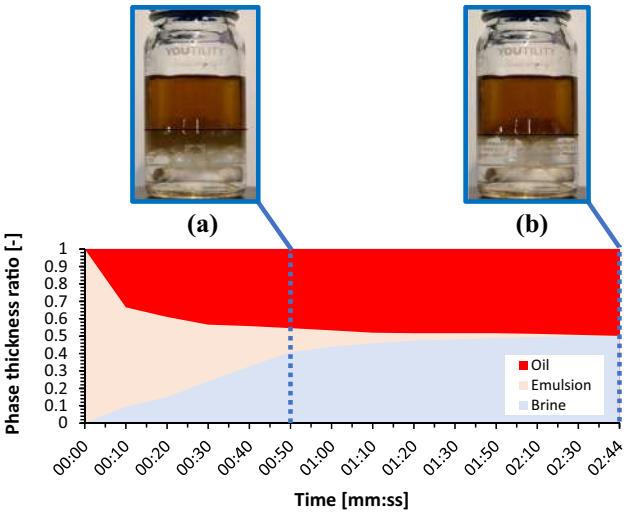

Fig. 4 Separation bottle depicting Exxsol D60 with 400 ppm crude oil, WC 50%—conditions of test bottle at **a** t_{in} and **b** $t_{sep.}$ In **b**, the small traces of oil in the water layer are oil remains that are stuck to the wall

of flow phenomena and established inlet flow patterns are gathered for supplementary analysis (Keleşoğlu et al. 2015).

The water cuts of each feed line were calculated by Eq. (1).

$$\mathrm{WC_i} = \frac{\rho_i - \rho_o}{\rho_w - \rho_o} \tag{1}$$

where ρ_i, ρ_o and ρ_w are initial, oil and water densities, respectively. Besides, the water cut of the inlet stream is determined using Eq. (2).

$$\mathrm{WC_{in}} = \frac{\mathrm{WC_1}\dot{Q}_1 + \mathrm{WC_2}\dot{Q}_2}{\dot{Q}_1 + \dot{Q}_2} \tag{2}$$

where $\dot{Q}_1$ and $\dot{Q}_2$ are the volumetric flow rates through the corresponding feed lines and $\mathrm{WC_1}$ and $\mathrm{WC_2}$ are the calculated water cuts of the water and Exxsol D60 feed lines. In the experiments, the water cut of the water line is practically equal to one and the water cut of the oil line is practically equal to zero. However, this calculation accounts for possible contamination of the pure water and pure oil lines with oil and water, respectively, due to poor separation in the storage tank. Separation efficiencies are estimated and reported at fixed extraction rates, (ER), as shown in Eq. (3).

$$\mathrm{ER} = \frac{\dot{Q}_3}{\dot{Q}_1} \tag{3}$$

where $\dot{Q}_3$ is flow rate through the water return/extraction line and $\dot{Q}_1$ is the mixed incoming flow rate through the water feed line. The separation efficiency is calculated by dividing

Table 2 Experimental variables of bottle tests

Study variables	Values	Fixed variables	Values	Response variables
1st series of bottle tests				
Water cut [%]	30, 50, 70 and 90	Fluid system	Crude oil–salt water	Separation time t_{sep} [s]
		Temperature [°C]	60	
		Rotation [rpm]	750	
		Rotation time [s]	30	
2nd series of bottle tests				
Crude spiking concentration [ppm]	200, 300, 400, 500, 600, 700 and 800	Fluid system	Exxsol D60—salt water	Separation time t_{sep} [s]
		Temperature [°C]	25	Interface stabilized time t_{in} [s]
		Rotation [rpm]	750	
Water cut [%]	25, 50 and 75	Rotation time [s]	30	

the rate of water extraction by the potential amount of water that can be removed at a certain ER. Equation (4) gives the expression.

$$\varepsilon = \frac{\mathrm{WC}_3 \dot{Q}_3}{\mathrm{ER}\left(\mathrm{WC}_{\mathrm{in}}\left(\dot{Q}_1 + \dot{Q}_2\right)\right)} \tag{4}$$

As previously stated, phase contamination will occur over time, with small amounts of Exxsol D60 dispersed in the inflow water and vice versa. The value of separation efficiency might become greater than 1 because of this. Therefore, in addition to separation efficiency, another indicator was calculated equal to the ratio of the water cut at the water extraction line by the WC at the water input line (Eq. 5). If this ratio is equal to one, this indicates good separation efficiency.

$$\mathrm{WC}_{\mathrm{ratio}} = \frac{\mathrm{WC}_3}{\mathrm{WC}_1} 100 \tag{5}$$

The study variables are:

- Three different crude spiking concentrations (1. no crude spiking, 2. the optimum crude spiking concentration which is gained from bottle tests results and 3. almost half concentration of optimum value to confirm performance behavior of separator). The first campaign (no crude spiking) is performed by Skjefstad and Stanko (2019), and this study repeated the same campaign for benchmarking.
- Four different inlet water cuts (30, 50, 70 and 90) to deal with wide range of emulsions.
- Nine total flow rates to cover different types of flow regimes.
- Three different extraction rates to examine effect of water extraction quantity on separator performance.

The basic fluid system is Exxsol D60 and 3.4 wt% NaCl salt water, and the temperature of the experiments is set to 25 °C. Designed experimental campaigns report separation efficiency, water cut ratio, flow pattern at inlet of MPPS and alteration of phases thickness inside the separator for each flow condition. Table 3 presents the test matrix with specified fixed, study and response variables for separation performance tests.

The flow pattern was determined by using photographs taken from "Introduction" section in Fig. 5. The following subsections present the separation performance results. In

Table 3 Experimental campaign test matrix

Separation performance tests				
Study variables	Values	Fixed variables	Values	Response variables
Water cut [%]	30, 50, 70 and 90	Fluid system	Exxsol D60 & 3.4*wt*% NaCl salt water	Separation efficiency [%]
Crude spiking concentration [ppm]	0, 185 and 400			Water cut ratio [%]
		Temperature [°C]	25	Flow pattern at inlet
Flow rate [L/min]	300, 350, 400, 450, 500, 550, 600, 650 and 700			Phase thickness [in]
Extraction rate [%]	50, 70 and 90			

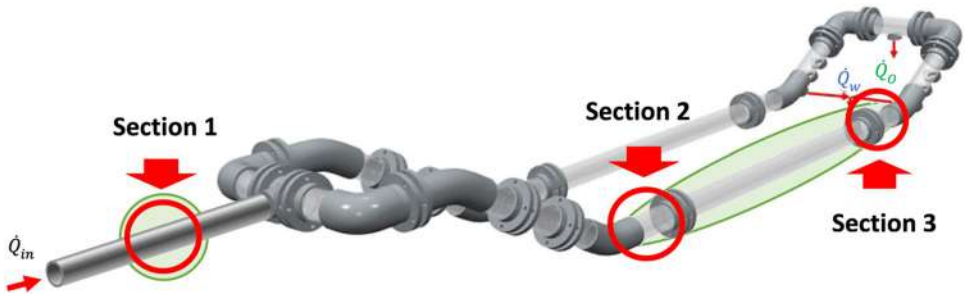

Fig. 5 Visual inspection on separation process

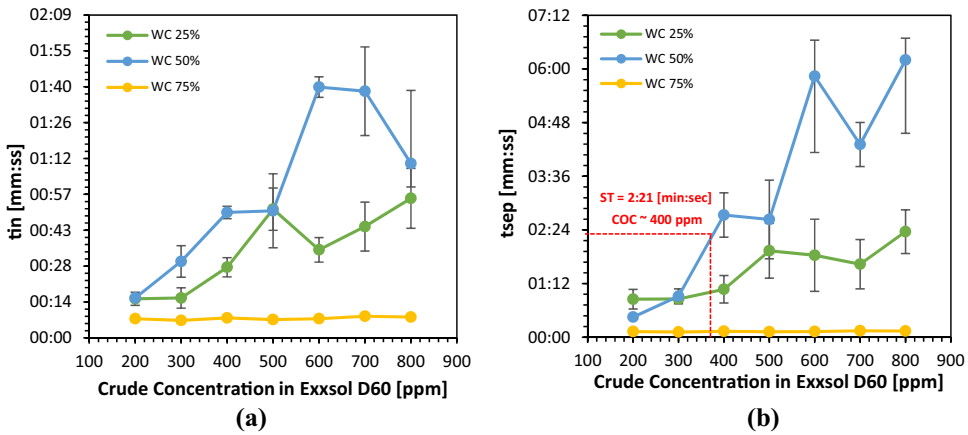

Fig. 6 **a** Required time for fixed interface, t_{in}, **b** required time for phase separation, $t_{sep,}$ versus concentration of crude oil in the spiked Exxsol D60

addition, the variation of phases thickness within the separator is recorded by cameras which take photographs from Sections 2 and 3.

Results and discussion

Bottle test

The measured separation times are presented in Fig. 6, for several water fractions and for different concentrations of spiked oil. The temperature was kept constant at 25 °C. For water cuts equal to 50% and 25%, increasing the concentration of crude oil in Exxsol D60 gives a significant increase in both t_{in} and t_{sep} with respect to the values for pure Exxsol D60 and salt water. The relationship between t_{in} and t_{sep} versus crude concentration is non-monotonic. For a WC equal to 75%, there was no noticeable change in t_{in} nor in t_{sep} when the crude is spiked.

The measured separation time, (t_{sep}), for a mixture of pure crude oil and salt water for four different water cuts at a temperature of 60 °C is illustrated in Fig. 7. The results show that a decrease in the water cut gives higher t_{sep}. For example, when varying the water cut from 50 to 25%, the t_{sep} increases from 2 min and 21 s to 11 min and 38 s. This observation may indicate that the formed emulsion layer after stirring is more stable for the 25% water cut.

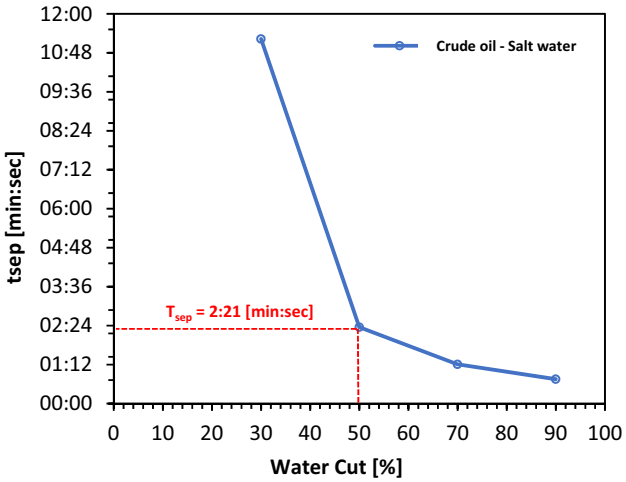

Fig. 7 Effect of water cut on separation time of crude oil and salt water mixture

To select the proper spiking concentration such that the separation characteristics of the spiked Exxsol D60 and salt water mixture at ambient temperature are similar to the crude oil and salt water mixture at high temperature, it was decided to use a crude oil concentration that would give the same separation time as the crude oil and salt water mixture at a water cut of 50%. It was decided to use a water cut of 50% because the separator is meant for

water-dominated flow regimes, and 50% was the case that exhibited the worst separation performance. The mixture of crude oil and salt water at 50% water cut has a separation time of 2 min and 21 s. A crude spiking concentration close to 400 ppm was then selected because it can provide similar separation times.

The mixing and shear stress conditions of bottle tests and flow in pipes are usually different; therefore, it could be that the separation times in the separator will be significantly different from the ones measured in the separation prototype. To address this uncertainty and avoid ending up with a fluid mixture that is too difficult to separate, the crude spiking was performed in two steps: first, one with 185 ppm and then one with 400 ppm. Photographs of spiked Exxsol D60 with salt water for several crude oil concentrations are shown in Fig. 8. These images show that adding 400 ppm crude spiking to Exxsol D60 will not affect the visibility significantly. Similar visibility results were obtained when using acrylic pipes, which are the same material that the separation prototype is made of.

Separation performance test

The results of the performance separation study are presented in the subsections below. In the first subsection, the flow pattern map just upstream of the MPPS inlet is reported. Then, the separation efficiency and water cut ratio of each flow condition are presented and compared with each other. The results include color maps of the separation performance and water cut ratio as a function of water cut and inlet flow rates, for several values of extracted rates (Table 3). Next, the variation of phases thickness within the horizontal section of separator is investigated. The results also include images and measurements of the thickness of the fluid layers taken at Sections 2 and 3 (Fig. 5). Finally, the extraction criteria to guarantee a successful separation with MPPS are discussed.

Flow pattern map

Six different liquid–liquid flow patterns were observed during the separation performance tests. The flow patterns were identified using the convention presented by Rivera et al. (2008). Some details about the flow pattern description and acronyms used are presented in "Appendix" section. The flow pattern map for the Exxsol D60 and salt water mixture (Skjefstad and Stanko 2019) and the mixture of spiked Exxsol D60 (400 ppm) and salt water are shown in Fig. 9. When the flow rate is low, the oil and water phases are continuous, but when the flow rate rises, there is enough energy to cause the phases to separate into droplets (Martin Brown and Dejam 2022). Adding a small amount of crude spiking did not change the transitions of the patterns dramatically, but there some are minor differences. The area of the flow pattern dispersion of water in oil and dispersion of oil water (Dw/o + Do/w) is larger with crude spiking when compared to the unspiked fluids. For example, at a rate of 700 L/min, the flow pattern transition for the unspiked oil is at a water cut of 30%, while for the spiked oil it occurs at a water cut 30%. This means the inversion point is changed from 40 to 30%. Crude oil spiking seems to cause more stable dispersion layers and mixing.

Performance mapping

Figure 10 shows color maps of calculated values of separation efficiency and water cut ratio for several combinations of total flow rate and water cut, following the test matrix presented in Table 3. These plots are for the unspiked oil and salt water mixture which were reported by Skjefstad and Stanko (2019). Several color maps are provided depending on the extraction rate. It is clear from the data that separation efficiency declines when the water cut is dropped, and the extraction rate is increased. The water cut range between 30 and 50% poses the greatest challenge for operation, and in this range both the extraction rate and inlet flow rate must be reduced for better separation performance. The minimum

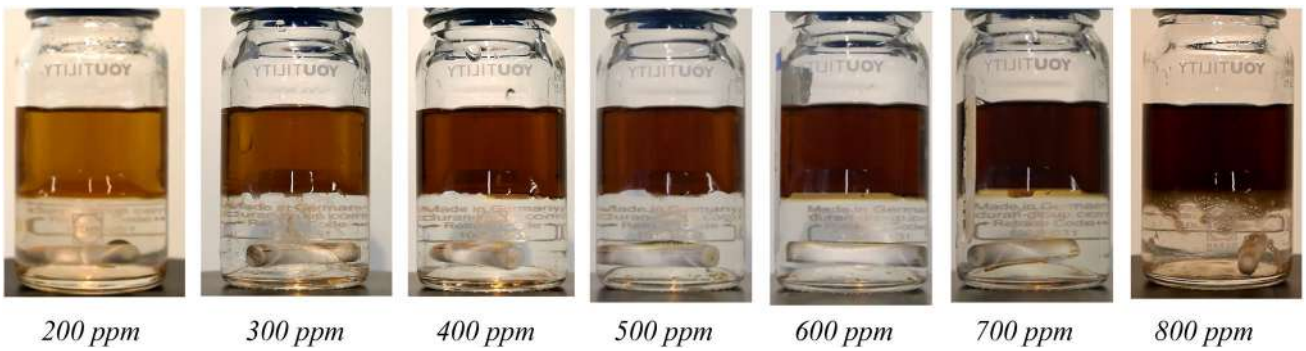

Fig. 8 Visibility test

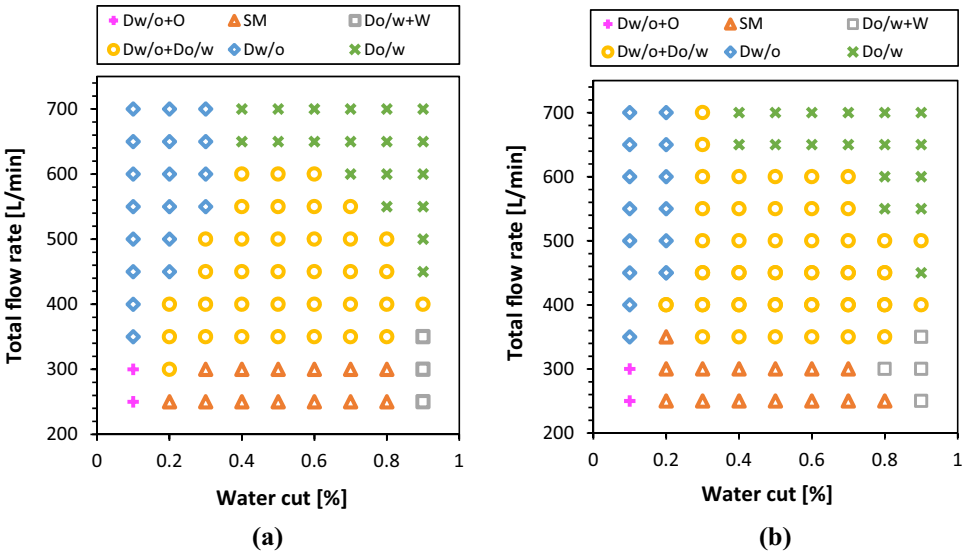

Fig. 9 Established flow pattern map at the MPPS inlet **a** Exxsol D60 without crude spiking (Asaadian et al. 2022; Skjefstad and Stanko 2019), **b** Exxsol D60 with 400 ppm crude spiking

separation efficiency of 78.8% is achieved when Qt = 700 L/min, WC = 30% and ER = 90%. The highest separation efficiency is achieved in the low total flow rate and high WC area, where numerous test points reach 100% separation efficiency.

The errors associated with the efficiency values vary somewhat depending on the value of the efficiency but are low. For example, the operating point Qt = 300 L/min, WC = 30%, ER = 50%, yields a maximum efficiency error of ± 0.71 pp. At Qt = 700 L/min, WC = 90% and ER = 90%, the error associated with separation efficiency is ± 0.35 pp (Ohrem et al. 2019). Because the oil and water content in a stream are determined using Coriolis flowmeters, it is not possible to detect very small amounts of oil in water or vice versa, because they usually fall within the measurement error. The error values depend on the flow conditions and water cut, but, for example, concentrations of oil in the water outlet of around 2000 ppm could pass unnoticed, because of the measurement error. For all operating points, the cutoff in the WC ratio is roughly 99% ± 0.35 pp (Skjefstad et al. 2020). Table 4 presents values of total inlet rate and WC that bound the region with high separation efficiency for each ER (separator operational envelope). High efficiency in this context is defined as points that have a separation efficiency equal or higher than 98%.

Figure 11 shows color maps of the separation efficiency and water cut ratio for several combinations of total flow rate and water cut, following the test matrix presented in Table 3. These plots are for the Exxsol D60 + 185 ppm crude spiking and 3.4 wt% NaCl water mixture. Several color maps are provided depending on the extraction rate. Adding 185 ppm of crude spiking causes a significant drop in separation performance with respect to the unspiked crude-saltwater mixture, especially for points at low water cuts (30 to 50%) and high flow rates. The same trend is noticeable in the water cut ratio color maps. The minimum efficiency dropped to 44.8% for total flow rate 700 L/min, water cut 30% and extraction rate of 90%.

Table 5 presents values of total inlet rate and WC that bound the region with high separation efficiency for each ER (separator operational envelope). High efficiency in this context is defined as points that have a separation efficiency equal or higher than 98%. The operation envelope of the separator has shrunk considerably from the one for unspiked oil and salt water.

Figure 12 shows color maps of the separation efficiency and water cut ratio for several combinations of total flow rate and water cut, following the test matrix presented in Table 3. These plots are for the Exxsol D60 + 400 ppm crude spiking and 3.4 wt% NaCl water mixture. Several color maps are provided depending on the extraction rate. Adding 400 ppm of crude spiking causes a significant drop in separation performance with respect to the unspiked crude–saltwater mixture, especially for points at low water cuts (30 to 50%) and high flow rates. Points with water cuts higher than 90% still maintain their efficiency higher that 98%.

The color maps of the water cut ratio show there is considerable oil contamination in the tapped water flowline for extraction rates of 70 and 90% and flow rates higher than 500 L/min. The minimum efficiency registered is 39.87% which corresponds to a water cut of 30% (minimum) and the flow rate and extraction rate 700 L/min and 90%, respectively (maximum values).

Table 6 presents values of the total inlet rate and WC that bound the region with high separation efficiency for each ER (separator operational envelope). High efficiency in this context is defined as points that have a separation efficiency equal or higher than 98%. The operation

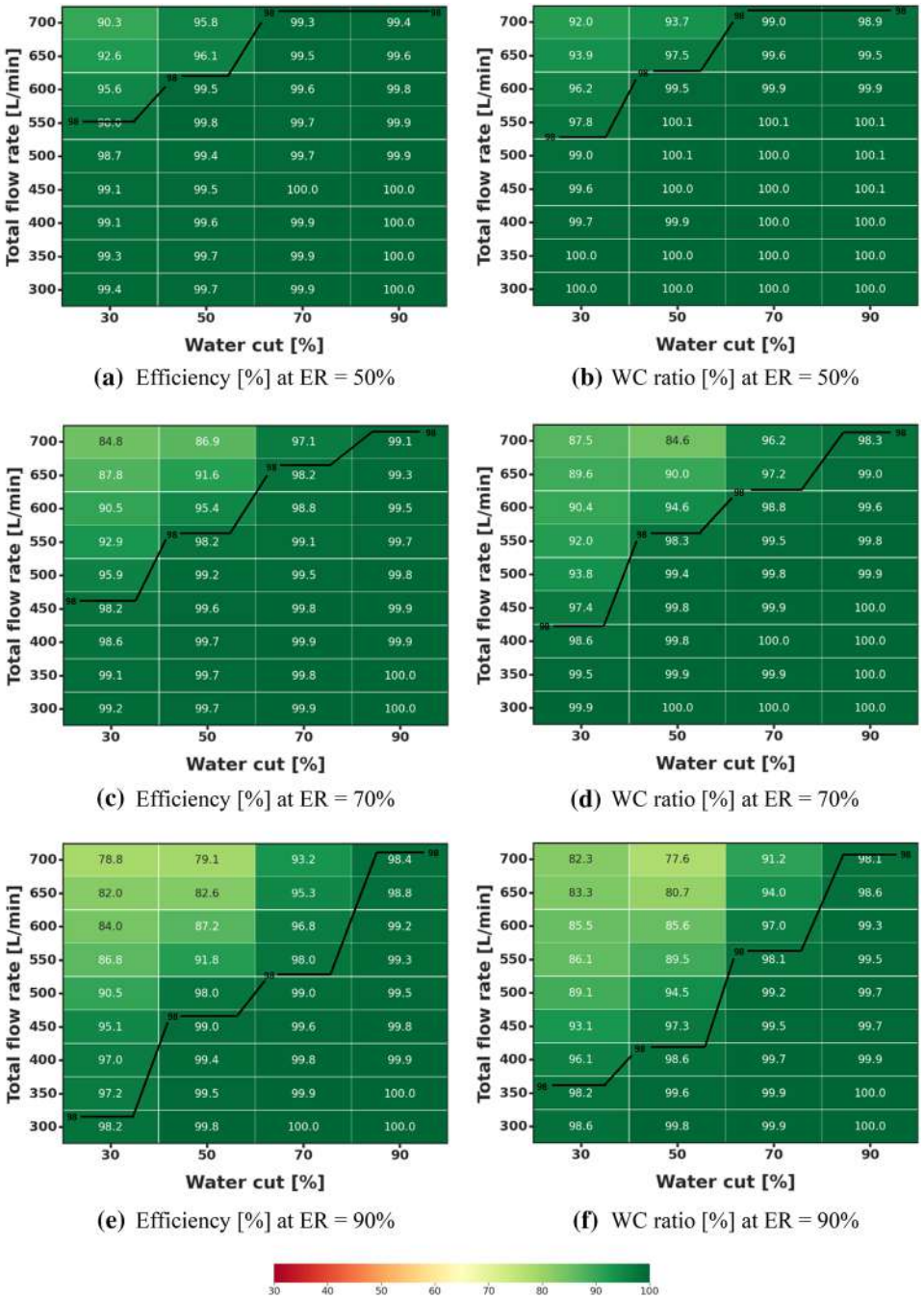

Fig. 10 Separation efficiency and water cut ratio results for Exxsol D60 and 3.4 wt% NaCl water (Skjefstad and Stanko 2019)

Table 4 Operation envelope for Exxsol D60 & 3.4 *wt%* NaCl water (Skjefstad and Stanko 2019)

ER [%]	$\dot{Q}_t\,[L/\min]\ (U_m[\mathrm{m/s}])$			
	30% WC	50% WC	70% WC	90% WC
50	550 (0.26)	600 (0.28)	700 (0.33)	700 (0.33)
70	450 (0.21)	550 (0.26)	650 (0.30)	700 (0.33)
90	300 (0.14)	450 (0.21)	550 (0.26)	700 (0.33)

envelope of the separator has shrunk considerably with respect to the one for spiked oil (185 ppm or crude) and salt water.

In general, oil continuous flow regimes are affected most by spiking and this effect is harsher around 30% water cut where it was stated as the inversion point of water and oil emulsion on the flow pattern map at the inlet of the MPPS.

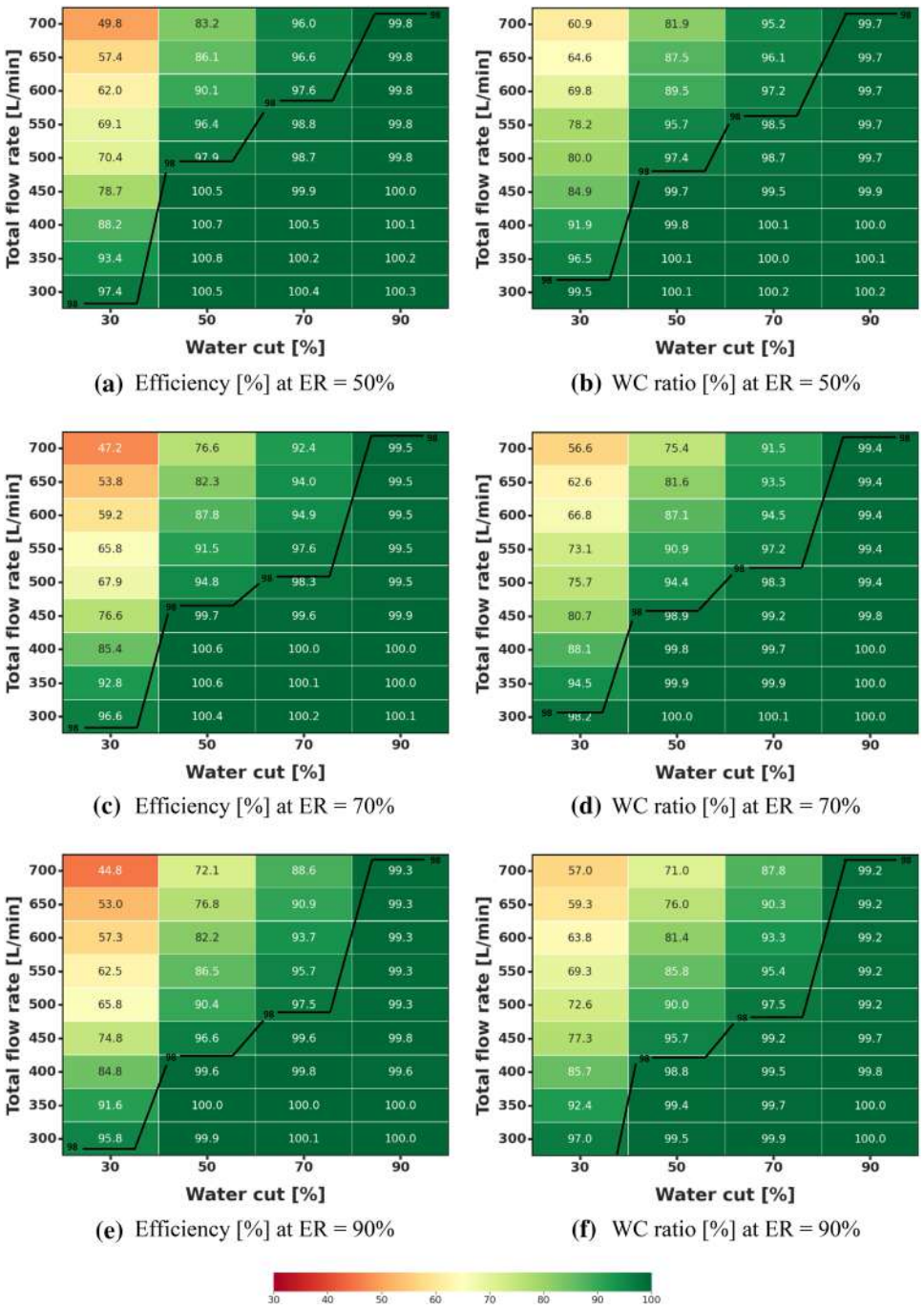

Fig. 11 Separation efficiency and water cut ratio for Exxsol D60 (+185 ppm crude spiking) and 3.4 wt% NaCl water

Table 5 Operation envelope for Exxsol D60 (+185 ppm crude spiking) and 3.4 wt% NaCl water

ER [%]	$\dot{Q}_t[L/\min]$ $(U_m[\mathrm{m/s}])$			
	30% WC	50% WC	70% WC	90% WC
50	300 (0.14)	500 (0.23)	600 (0.28)	700 (0.33)
70	< 300 (0.14)	450 (0.21)	500 (0.23)	700 (0.33)
90	< 300 (0.14)	400 (0.19)	500 (0.23)	700 (0.33)

Phase thickness

In this subsection, the variation of the thickness of the fluid phase layers at the inlet (Section 2) and outlet (Section 3) of the horizontal pipe section of the MPPS is investigated for several combinations of inlet flow rates and water cuts. All the measurements are taken by visual inspection and image analysis by ImageJ software. As illustrated in Fig. 13, three distinct layers of oil, emulsion

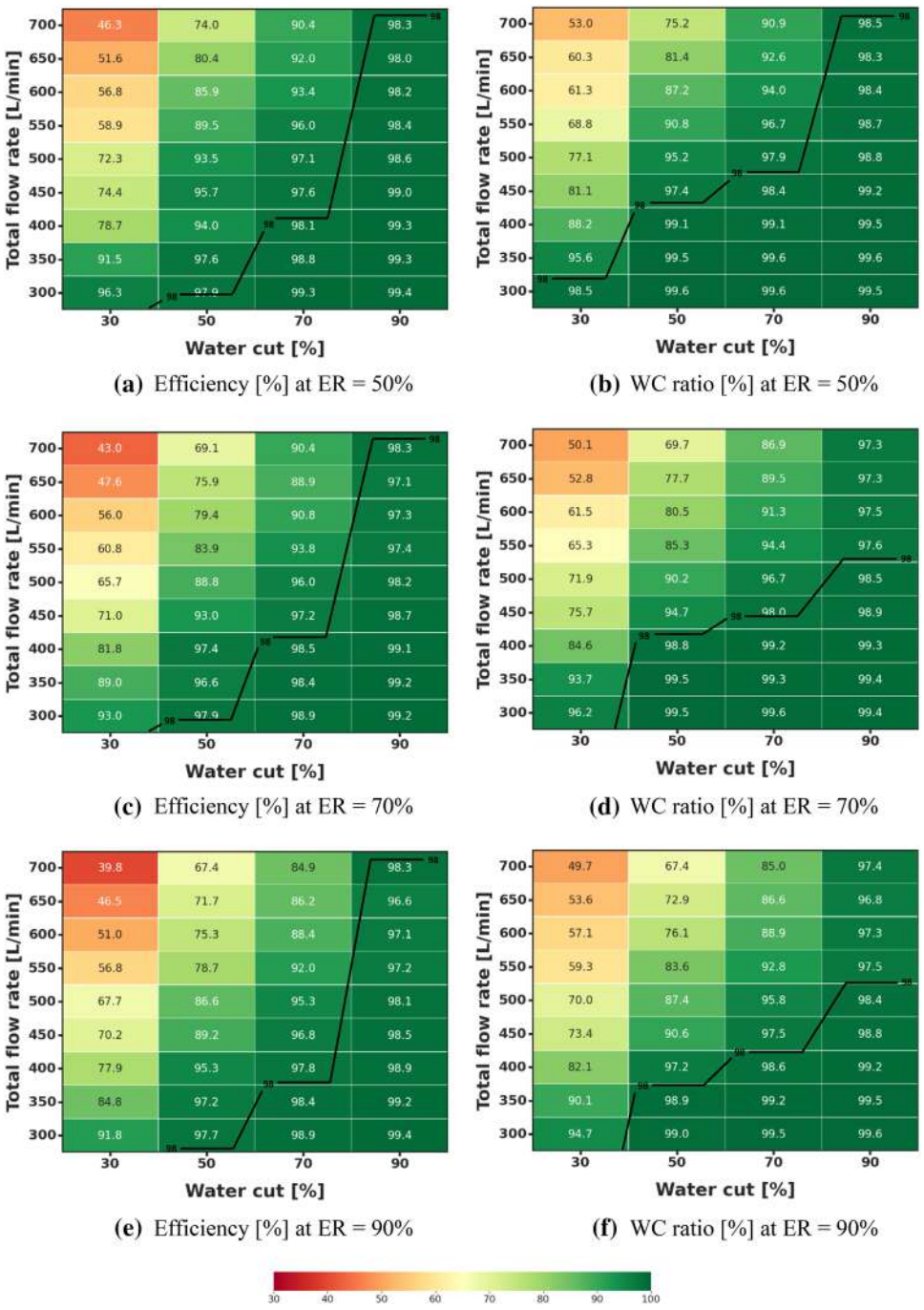

Fig. 12 Separation efficiency and water cut ratio for Exxsol D60 (+400 ppm crude spiking) & 3.4 wt% NaCl water

Table 6 Operation envelope for Exxsol D60 (+400 ppm crude spiking) and 3.4 wt% NaCl water

ER [%]	$\dot{Q}_t[L/\min]$ $(U_m[\mathrm{m/s}])$			
	30% WC	50% WC	70% WC	90% WC
50	< 300 (0.14)	300 (0.14)	400 (0.19)	700 (0.33)
70	< 300 (0.14)	300 (0.14)	400 (0.19)	700 (0.33)
90	< 300 (0.14)	< 300 (0.14)	400 (0.19)	700 (0.33)

and salt water are detected in all the established flow patterns in the horizontal pipe section.

In Fig. 14 the evolution of the phase thicknesses is presented for a total flow rate 300 L/min and extraction rate of 90%. Four different water cuts were tested (Fig. 14a–d). The thickness of the emulsion layer is reduced considerably at the end of the horizontal section for water cuts of 50, 70 and 90%. However, it remains relatively stable for a water cut of 30%.

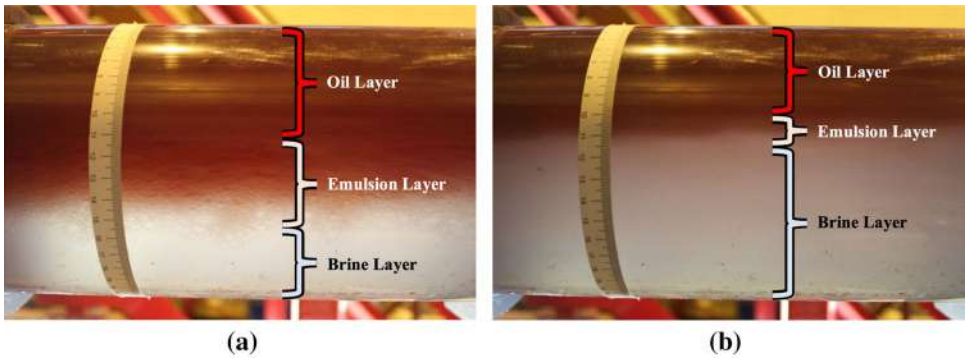

Fig. 13 Phase thickness determination by visual inspection, **a** in O + Do/w + Dw/o + W, **b** SM

Figure 14e–h displays the thickness of the fluid layers at Sections 2 and 3, as a function of the water cut. In Section 2, the thickness of the emulsion layer increases slightly when the water cut increases. In Section 3 the opposite trend is observed. The dissolving of the emulsion layer causes an increase in the oil and brine thickness at Section 3. At 30% water cut the thickness of the oil layer increases, mainly due to the breakdown of the emulsion layer. For higher water cuts, the breakdown of the emulsion layer increased the thickness of both oil and brine layers. Generally, a thick water layer forms quicker than the oil layer in high water cuts (e.g., 70 and 90%); meanwhile, the trend is inverted for low water cuts. The estimated residence time is 20 s for a total flow rate of 300 L/min. As it is illustrated in the above figures, a residence time equal to 20 s for all water cuts is enough to induce the formation of a noticeable brine layer that can be subsequently drained.

Figure 15a–h presents similar plots as Fig. 14 but for a total flow rate of 500 L/min. The thickness of the emulsion layer is somewhat reduced at the end of the horizontal section, but it does not disappear completely for any water cut value. It remains relatively stable for the water cut of 30%. At the end of the horizontal section (Section 3), a noticeable clear layer of brine is formed for water cuts ranging between 50 and 90%.

Figure 15e–h illustrates the thickness of the fluid layers at Sections 2 and 3, as a function of the water cut. In Section 2, the thickness of the formed emulsion layer is highest for the 90% water cut and then it decreases with a decline in the water cut. The same behavior is observed at Section 3. The estimated residence time is decreased to 12 s for total flow rate 500 L/min. This residence time is not enough to ensure the formation of a clean brine layer for a low water cut of 30%.

Figure 16 presents similar plots as Fig. 14, but for a total flow rate of 700 L/min. Increasing the total flow rate to 700 L/min results in shorter residence time for fluids in the horizontal pipe section (8 s). As presented in Fig. 16a–d, the emulsion layer thickness does not change significantly from Section 2 to Section 3, although a clean salt water layer forms at water cuts 70 and 90%.

Figures 15, 16e–h show the thickness of the fluid layers at Sections 2 and 3, as a function of the water cut. A high fraction of water at water cut 90% used bouncy force to create a thicker layer of clear brine at Section 3. Due to low residence time, the thickness of the oil, brine and emulsion layers is relatively stable for water cuts from 30 to 70%.

From the presented results, it seems that the current horizontal length of the separator is not enough to ensure the complete separation of the emulsion layer except for the lowest total flow rate (300 L/min). Also, for water cuts equal to 30% and all total flow rates, the emulsion layer is relatively stable and does not separate significantly, so it is unclear whether a longer horizontal section will allow full separation. However, for almost all cases, the horizontal section promoted the formation of a layer of clean salt water at the bottom of the pipe. This layer can be drained, giving high values of water cut ratio.

To further explore what parameters affect the efficiency of the separator, a dimensionless brine characteristic (BC) number is defined (Eq. 6).

$$\mathrm{BC} = \left(\frac{V_{\mathrm{brine}}}{V_{\mathrm{mix}}}\right)\left(\frac{t_{\mathrm{r}}}{t_{\mathrm{sep}}}\right) \tag{6}$$

where this number contains the amount of brine (V_{brine}) present in the fluid (in volume basis) (V_{mix}) and the ratio between the residence time (t_{r}) in the separator and the required separation time (t_{sep}), from the bottle tests. Figure 17 was prepared to depict the separation efficiency versus the brine characteristic number. This chart seems to indicate that there is a certain minimum amount of brine characteristic necessary (0.01) to result in separation efficiency values higher than 98%. The relation between separation efficiency and brine characteristic lower than 0.01 can be fitted on a logarithmic trendline with acceptable accuracy.

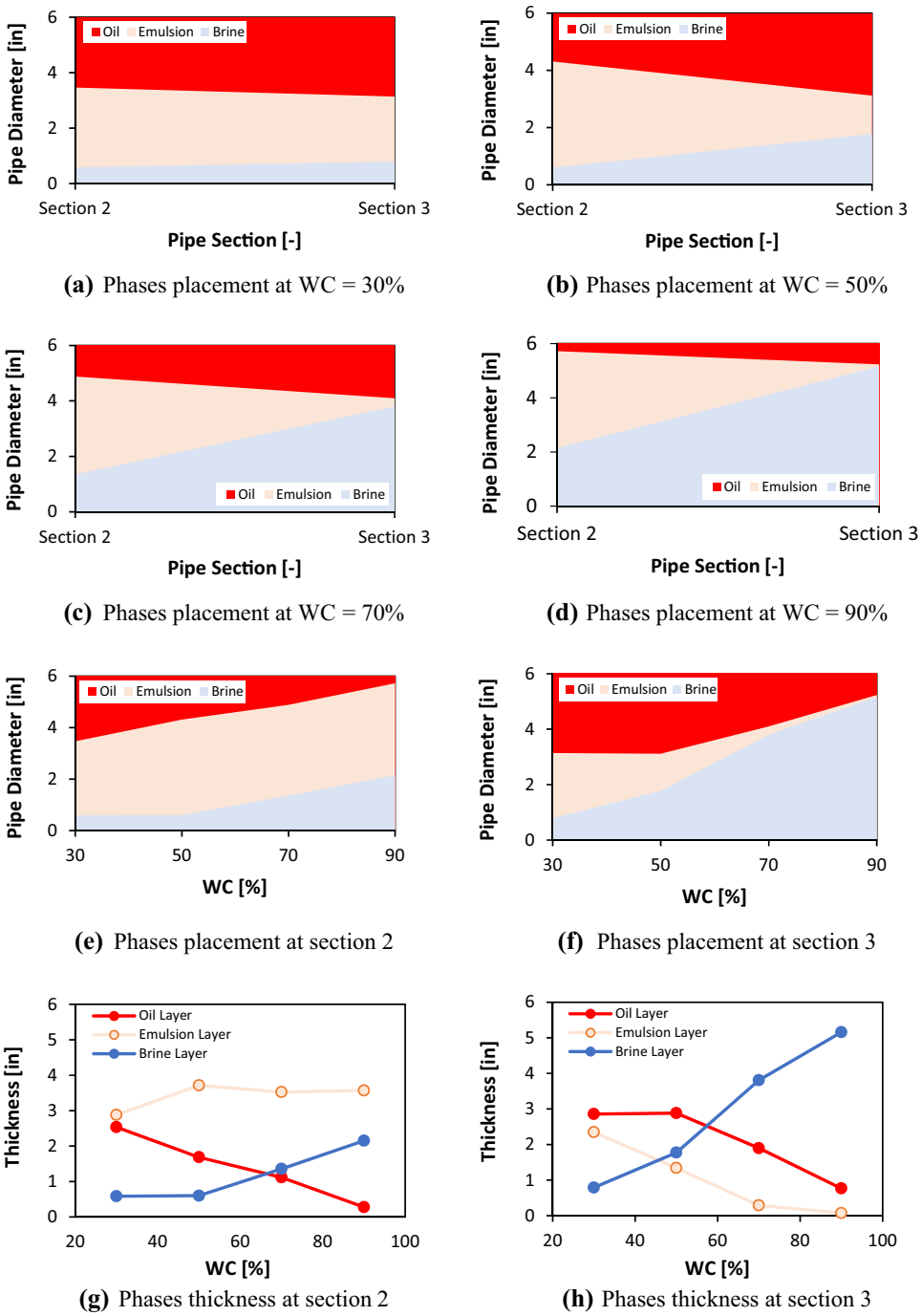

(a) Phases placement at WC = 30%

(b) Phases placement at WC = 50%

(c) Phases placement at WC = 70%

(d) Phases placement at WC = 90%

(e) Phases placement at section 2

(f) Phases placement at section 3

(g) Phases thickness at section 2

(h) Phases thickness at section 3

Fig. 14 Phases placement and thickness for total flow rate = 300 [L/min] and ER = 90%

Summary and conclusions

The following conclusions can be drawn from presented results:

- The spiking process can be utilized to mimic the characteristics of real crude oil mixtures and aid in extrapolating experimental results to real field conditions.
- The multi-parallel pipe separator shows acceptable separation performance in water continuous flow patterns. With decreasing inlet WC and increasing extraction rate and total flow rate, separation performance decreases.
- Appearance of more frequent dispersion flow patterns in experiment matrix in case of suing spiking agent shows crude oil spiking leads to more stable dispersion layers and mixing.
- The introduction of spiking agent reduced separation efficiency in oil continuous flow regimes significantly up to 49% due to a more stable emulsion layer than in unspiked flow conditions.

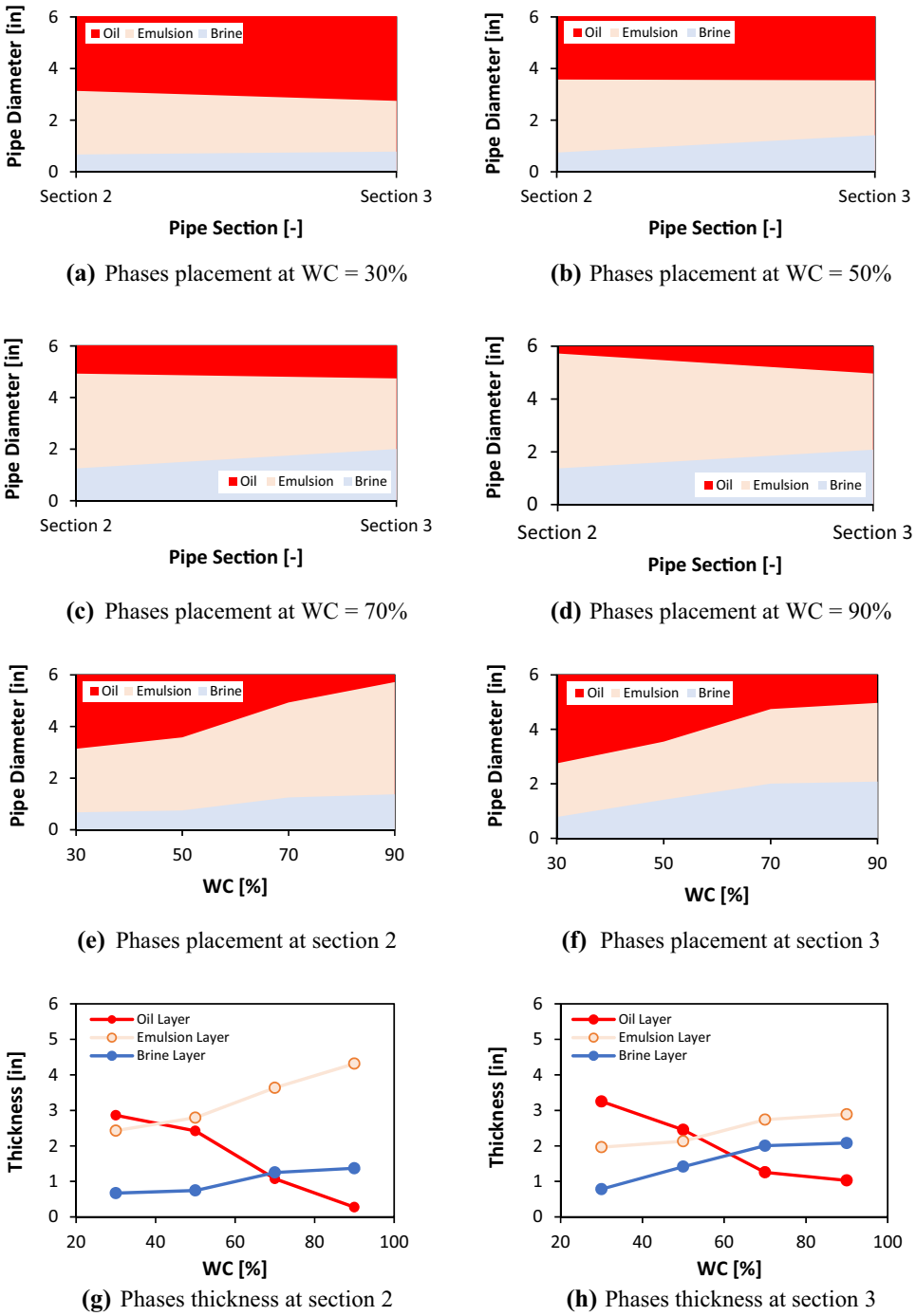

(a) Phases placement at WC = 30%

(b) Phases placement at WC = 50%

(c) Phases placement at WC = 70%

(d) Phases placement at WC = 90%

(e) Phases placement at section 2

(f) Phases placement at section 3

(g) Phases thickness at section 2

(h) Phases thickness at section 3

Fig. 15 Phases placement and thickness for total flow rate = 500 [L/min] and ER = 90%

- The decrease in separation efficiency in the 30–50% WC range is due to a persistent emulsion layer in the separator and a lack of a thick layer of water. Lower total flow rate for this range of WC results in longer residence time, thicker water layer and, ultimately, improved separation efficiency.
- The separation efficiency directly depends on amount and quality of extracted water. The dimensionless brine characteristic number reflects both parameters to ensure efficient separation.

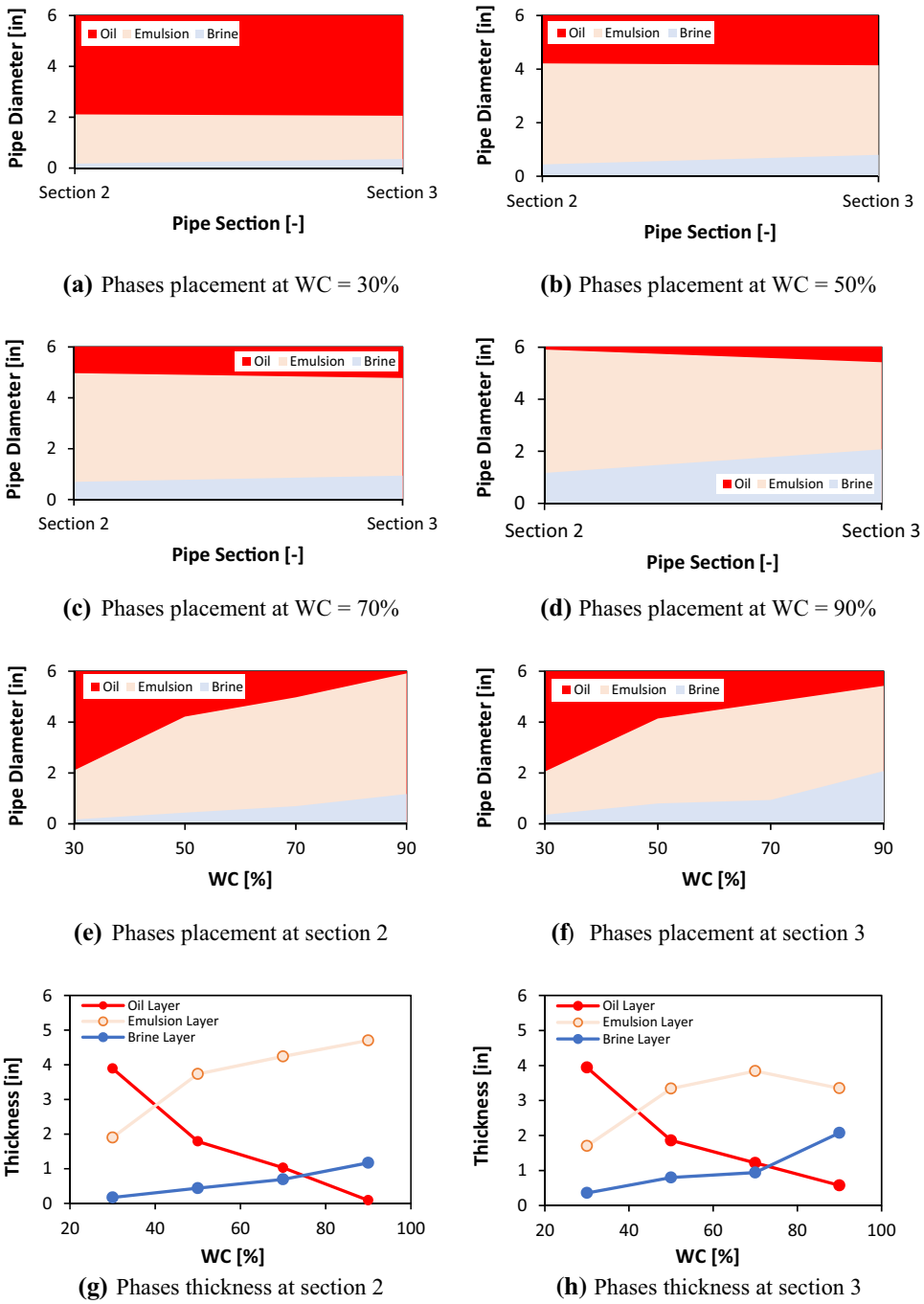

(a) Phases placement at WC = 30%

(b) Phases placement at WC = 50%

(c) Phases placement at WC = 70%

(d) Phases placement at WC = 90%

(e) Phases placement at section 2

(f) Phases placement at section 3

(g) Phases thickness at section 2

(h) Phases thickness at section 3

Fig. 16 Phases placement and thickness for total flow rate = 700 [L/min] and ER = 90%

Appendix: Characterization of different flow patterns in liquid–liquid pipe flow

Oil dispersion in water: [Do/w]

This flow configuration is created by high water superficial velocities and low to medium oil superficial velocities (e.g., 0.4 m/s). Shear forces break down the oil into small droplets, which then distribute throughout the cross section of the pipe. Depending on the fluid flows, the volume and size of the droplets may vary significantly. The mixing velocity profile is parabolic and generally centered within the pipe axis, as expected for single-phase flow (Fig. 18) (Rivera et al. 2008).

Dispersion of oil in water and water: [Do/w and W]

The turbulence forces in the mixture are lowered when the amount of water in the mixture is reduced (from Do/w), allowing oil droplets to coalescence and expand in size.

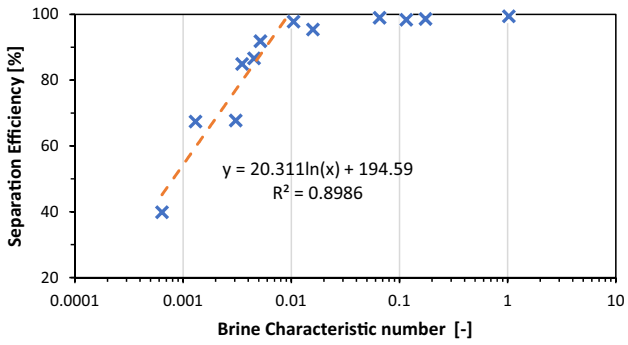

Fig. 17 Effect of the brine layer thickness ratio on separation efficiency

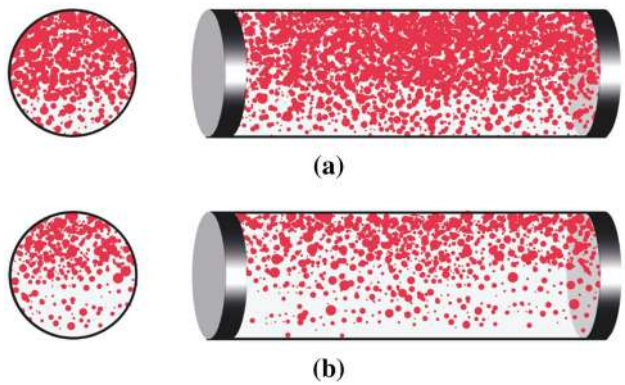

Fig. 18 Dispersion of oil in water [Do/w]. **a** High oil fraction, **b** low oil fraction

Fig. 19 Dispersion of oil in water and water [Do/w and W]

Fig. 20 Oil and dispersion of water in oil [O and Dw/o]

The distribution of the oil droplets is controlled by buoyancy forces, which push them to the top of the pipe, producing a clear (or almost transparent) water layer at the bottom (Fig. 19) (Rivera et al. 2008).

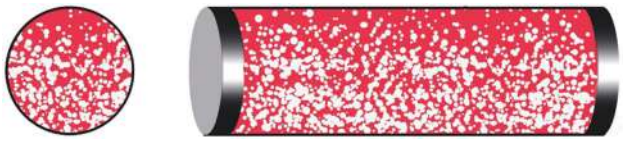

Fig. 21 Dispersion of water in oil [Dw/o]

Fig. 22 Stratified flow of water and oil [SM]

Oil and dispersion of water in oil: [O and Dw/o]

This structure is separated into two layers, one of which is dominated by oil and the other by water. Most of the upper section of the pipe is made up of oil. The lower half of the pipe features a dual dispersion. A dispersion of water in oil is observed over an oil in water dispersion. Due to the large degree of turbulence, this dual dispersion looks as a foam-like layer (Fig. 20) (Rivera et al. 2008).

Dispersion of water in oil: [Dw/o]

This is the only flow pattern in which the oil phase is continuous across the cross section of the pipe. Despite the fact that water is dispersed in the oil, it concentrated at the bottom of the pipe, forming a foam-like structure identical to the one described above (Fig. 21) (Rivera et al. 2008).

Stratified flow of water and oil: [SM]

This flow arrangement consists of two dominant, stratified and clear water and oil layers, and there may be a thin discernible dispersed/emulsion layer between the oil and water layers (Fig. 22) (Rivera et al. 2008).

Funding Open access funding provided by Norwegian University of Science and Technology. This work with project number of 237893, was done as a part of SUBPRO, a research-based innovation center for subsea production and processing. The Department of Geoscience and Petroleum, NTNU, the Research Council of Norway, and key industry partners all contributed financially to SUBPRO.

Declarations

Conflict of interest The authors declared that they have no conflicts of interest in this work.

Ethical approval We certify that this manuscript has never been published before and is not presently being considered for publication anywhere. This paper also reflects our own research.

References

Asaadian H, Harstad S, Stanko M (2022) Drainage potential curves of single tapping point for bulk oil–water separation in pipe. Energies 15(19):6911. https://doi.org/10.3390/en15196911

Asaadian H, Stanko M (2023) An experimental study on the effect of gas on the performance of a multi-parallel pipe oil-water separator (MPPS). InGas Oil Technol Showc Conf Onepetro. https://doi.org/10.2118/214062-MS

Boxall JA, Koh CA, Sloan ED, Sum AK, Wu DT (2010) Measurement and calibration of droplet size distributions in water-in-oil emulsions by particle video microscope and a focused beam reflectance method. Ind Eng Chem Res 49(3):1412–1418. https://doi.org/10.1021/ie901228e

Bringedal B, Ingebretsen T, Haugen K (1999) Subsea separation and reinjection of produced water. Offshore Technol Conf. https://doi.org/10.4043/10967-MS

Brown DE, Pitt K (1972) Drop size distribution of stirred non-coalescing liquid—liquid system. Chem Eng Sci 27(3):577–583. https://doi.org/10.1016/0009-2509(72)87013-1

Calabrese RV, Chang TP, Dang PT (1986) Drop breakup in turbulent stirred-tank contactors. Part I: effect of dispersed-phase viscosity. AIChE J 32(4):657–666. https://doi.org/10.1002/aic.690320416

Capela Moraes CA, da Silva FS, Marins LP, Monteiro AS, de Oliveira DA, Pereira RM, Pereira RD, Alves A, Raposo GM, Orlowski R, Figueiredo L (2012) Marlim 3 phase subsea separation system: subsea process design and technology qualification program. In: Offshore technology conference. OnePetro. https://doi.org/10.4043/23417-MS

da Silva FS, Monteiro AS, de Oliveira DA, Capela Moraes CA, Marins PM (2013) Subsea versus topside processing-conventional and new technologies. In: OTC Brasil. OnePetro. https://doi.org/10.4043/24519-MS

de Oliveira DA, Pereira RD, Capela Moraes CA, Baracho VP, de Souza RD, Euphemio ML, da Silva FS, Monteiro AS, Casanova CC, Duarte DG, Raposo GM (2013) Comissioning and startup of subsea marlim oil and water separation system. In: OTC Brasil. OnePetro. https://doi.org/10.4043/24533-MS

Fakhru'l-Razi A, Pendashteh A, Abdullah LC, Biak DR, Madaeni SS, Abidin ZZ (2009) Review of technologies for oil and gas produced water treatment. J Hazard Mater 170(2–3):530–551. https://doi.org/10.1016/j.jhazmat.2009.05.044

Fantoft R, Hendriks T, Elde J (2006) Technology qualification for the tordis subsea separation, boosting, and injection system. In: Offshore technology conference. OnePetro. https://doi.org/10.4043/17981-MS

Fossen M, Schümann H (2017) Experimental study of the relative effect of pressure drop and flow rate on the droplet size downstream of a pipe restriction. J Dispers Sci Technol 38(6):826–831. https://doi.org/10.1080/01932691.2016.1207184

Gramme PE, Haukom I, Inventors, Norsk Hydro ASA, Assignee (2009) Pipe separator for the separation of fluids, particularly oil, gas and water. United States patent US 7,516,794

Grave EJ, Olson MD (2014) Design and performance testing of a subsea compact separation system for deepwater applications. Oil Gas Facil 3(04):16–23. https://doi.org/10.2118/0814-0016-OGF

Gupta RK, Dunderdale GJ, England MW, Hozumi A (2017) Oil/water separation techniques: a review of recent progresses and future directions. J Mater Chem A 5(31):16025–16058. https://doi.org/10.1039/C7TA02070H

Hannisdal A, Westra R, Akdim MR, Bymaster A, Grave E, Teng DT (2012) Compact separation technologies and their applicability for subsea field development in deep water. In: Offshore technology conference. OnePetro. https://doi.org/10.4043/23223-MS

Horn T, Bakke W, Eriksen G (2003) Experience in operating world's first subsea separation and water injection station at troll oil field in the North Sea. In: Offshore technology conference. OnePetro. https://doi.org/10.4043/15172-MS

Keleşoğlu S, Rodionova G, Pettersen BH, Foss M, Sjöblom J (2015) Preparation and characterization of reference fluids to mimic flow properties of crude oil emulsions (w/o). J Dispersion Sci Technol 36(10):1458–1464. https://doi.org/10.1080/01932691.2014.996890

Martin Brown N, Dejam M (2022) An extensive scope of flow loops with a focus on particle transport. Phys Fluids 34(8):081301. https://doi.org/10.1063/5.0099309

Ohrem SJ, Skjefstad HS, Stanko M, Holden C (2019) Controller design and control structure analysis for a novel oil–water multi-pipe separator. Processes 7(4):190. https://doi.org/10.3390/pr7040190

Oil & Gas Association (2016) Environmental report—environmental work by the oil and gas industry, facts and development trends

Orlowski R, Euphemio ML, Euphemio ML, Andrade CA, Guedes F, Tosta da Silva LC, Pestana RG, de Cerqueira G, Lourenço I, Pivari A, Witka A (2012) Marlim 3 phase subsea separation system-challenges and solutions for the subsea separation station to cope with process requirements. In: Offshore technology conference. OnePetro. https://doi.org/10.4043/23552-MS

Pereyra E, Mohan RS, Shoham O (2013) A simplified mechanistic model for an oil/water horizontal pipe separator. Oil Gas Facil 2(03):40–46. https://doi.org/10.2118/163077-PA

Rivera RM, Golan M, Friedemann JD, Bourgeois B (2008) Water separation from wellstream in inclined separation tube with distributed tapping. SPE Proj Facil Constr 3(01):1–1. https://doi.org/10.2118/102722-PA

Sagatun SI, Gramme P, Horgen OJ, Ruud T, Storvik M (2008) The pipe separator-simulations and experimental results. In: Offshore technology conference. OnePetro. https://doi.org/10.4043/19389-MS

Shaiek S, Grandjean L (2015) SpoolSep for subsea produced water separation-experimental results. In: Offshore technology conference. OnePetro. https://doi.org/10.4043/25934-MS

Skjefstad HS, Stanko M (2017) Subsea water separation: a state of the art review, future technologies and the development of a compact separator test facility. In: 18th international conference on multiphase production technology. OnePetro

Skjefstad HS, Stanko M (2018) An experimental study of a novel parallel pipe separator design for subsea oil-water bulk separation. In: SPE Asia pacific oil and gas conference and exhibition. OnePetro. https://doi.org/10.2118/191898-MS

Skjefstad HS, Stanko M (2019) Experimental performance evaluation and design optimization of a horizontal multi-pipe separator for subsea oil-water bulk separation. J Pet Sci Eng 1(176):203–219. https://doi.org/10.1016/j.petrol.2019.01.027

Skjefstad HS, Dudek M, Øye G, Stanko M (2020) The effect of upstream inlet choking and surfactant addition on the performance of a novel parallel pipe oil–water separator. J Pet Sci Eng 189:106971. https://doi.org/10.1016/j.petrol.2020.106971

Stanko M, Golan M (2015) Simplified hydraulic design methodology for a subsea inline oil–water pipe separator. In: OTC Brasil. OnePetro

Stanko ME (2014) Topics in production systems modeling: separation, pumping and model based optimization.

Van Vu K, Fantoft R, Shaw CK, Gruehagen H (2009) Comparison of subsea separation systems. In: Offshore technology conference. OnePetro. https://doi.org/10.4043/20080-MS